JOURNAL OF Materials CHEMISTRY

Synthesis of TOPO-capped PtS and PdS nanoparticles from $[Pt(S_2CNMe(Hex))_2]$ and $[Pd(S_2CNMe(Hex))_2]$

M. Azad Malik,[a] Paul O'Brien*[b] and N. Revaprasadu[c]

[a]*Department of Chemistry, Imperial College of Science, Technology and Medicine, South Kensington, London, UK SW7 2AZ*
[b]*The Manchester Materials Science Centre and the Department of Chemistry, Manchester University, Oxford Rd, Manchester, UK M13 9PL. E-mail: paul.obrien@man.ac.uk*
[c]*Department of Chemistry, University of Zululand, Private Bag X1001, Kwadlangezwa, 3886, South Africa*

Received 15th May 2001, Accepted 17th October 2001
First published as an Advance Article on the web 26th November 2001

Bis(*n*-hexyl(methyl)dithiocarbamato)platinum(II) and bis(*n*-hexyl(methyl)dithiocarbamato)palladium(II) have been synthesised and characterised.

Both complexes have been used as precursors to grow thin films of PtS and PdS, respectively, on to GaAs substrates by the low pressure metal organic chemical vapour deposition (LP-MOCVD) method. The grown films were characterised by XRD, EDAX and SEM methods. These complexes are useful precursors for the growth of nanocrystals of PtS or PdS by thermolysis in trioctylphosphine oxide (TOPO). TOPO capped monodispersed nanoparticles of PtS (*ca.* 3 nm diameter) and PdS (*ca.* 5 nm diameter) have been prepared using the corresponding precursors. The PtS nanoparticles exhibit a strong excitonic peak at 360 nm in the absorption spectrum with the band edge at 410 nm. There is no visible excitonic peak in the absorption spectrum of the PdS nanoparticles with the band edge at 455 nm. The emission maxima of PtS (495 nm) and PdS (465 nm) are red shifted in relation to their band edges. XRD patterns showed both materials to exist in the tetragonal phase. The EDAX spectra show the presence of palladium and sulfur, and platinum and sulfur, with a strong peak for phosphorus due to TOPO.

Introduction

Platinum and palladium chalcogenides find applications in catalysis[1–5] and materials science.[6,7] The synthesis of thiocarbamato complexes of platinum and palladium from reaction of an aqueous solution of ammonium dithiocarbamate with platinum or palladium salts has been reported by Nakamoto[8] and Kuriacose[9] and we have now used these compounds as precursors for the preparation of metal sulfide nanoparticles and thin films.

PtS has been synthesized by the reaction of platinum(II) chloride, sulfur and sodium carbonate.[10] The reaction of tetrachloropalladate(II) with hydrogen sulfide is a route to palladium sulfide (PdS).[11] Organosols of PdS have been prepared by the reaction of the metal acetate with hydrogen sulfide.[12] Recently PdS has been synthesized from organochalcogenide-bridged dimeric 2-methylallylpalladium complexes.[13] The palladium chalcogenides were obtained by thermogravimetry, furnace decomposition and refluxing in xylene.

Here we report the synthesis of $[Pt(S_2CNMe(Hex))_2]$ and $[Pd(S_2CNMe(Hex))_2]$, their full characterisation and use as precursors to grow first TOPO capped PtS and PdS nanoparticles and then thin films of PtS and PdS by MOCVD (metal organic chemical vapour deposition).

Experimental

Chemicals

Sodium tetrachloroplatinate and sodium tetrachloropalladate were donated by Johnson Matthey. Tri-*n*-octylphosphine oxide; tri-*n*-octylphosphine and *N*-methylhexylamine were purchased from Aldrich Chemical Company Ltd and methanol, toluene from BDH. The solvents used for air-sensitive chemistry were distilled, deoxygenated under a nitrogen flow and stored over molecular sieves (type 4 Å, BDH) before use.

TOPO was purified by vacuum distillation at *ca.* 250 °C (0.1 Torr).

Instrumentation

UV/VIS absorption spectroscopy. A Philips PU 8710 spectrophotometer was used to carry out the optical measurements of the semiconductor nanoparticles. The samples were placed in silica cuvettes (1 cm path length).

Photoluminescence spectroscopy. A Spex FluoroMax instrument with a xenon lamp (150 W) and a 152 P photomultiplier tube as a detector was used to measure the photoluminescence of the particles. Good spectral data were recorded with the slits set at 2 nm and an integration time of 1 s. The samples were quantitatively prepared by dissolving 25 mg in 10 ml toluene. The samples were placed in quartz cuvettes (1 cm path length). The wavelength of excitation was set at a lower value than onset of absorption of a particular sample.

X-Ray diffraction (XRD). X-Ray diffraction patterns were measured using a Philips PW 1700 series automated powder diffractometer using Cu-K radiation at 40 kV/40 mA with a secondary graphite crystal monochromator. Samples were prepared on glass slides (5 cm). A concentrated toluene solution was slowly evaporated at room temperature on a glass slide to obtain a sample for analysis.

Electron microscopy. A JOEL 2000 FX MK 1 electron microscope operated at 200 kV with an Oxford Instrument AN

 DOI: 10.1039/b104226m

10000 EDS analyser was used for the conventional TEM (transmission electron microscopy) images. Selected area electron diffraction (SAED) patterns were obtained using a JEOL 2000FX MK 2 electron microscope operated at 200 kV. The samples for TEM and SAED were prepared by placing a drop of a dilute solution of the sample in toluene on a copper grid (400 mesh, Agar). The excess solvent was wicked away with a paper tip and completely dried at room temperature. EDAX (energy dispersion analytical X-ray) analysis was performed on samples deposited by evaporation on glass substrates by using a JEOL JSM35CF scanning electron microscope.

Other. NMR spectra were recorded using a Bruker AM250 pulsed Fourier transform instrument. Infrared spectra were obtained using a Matteson Polaris FT-IR spectrometer with samples as Nujol mulls. Mass spectra were recorded by a micromass Auto-spec-Q instrument using micromass OPUS software. An electron impact energy of 70 eV at 10^{-7} Torr was used to initiate mass fragmentation. Melting points were measured in sealed tubes with an electrothermal melting point apparatus and are uncorrected. Microanalyses were carried out by the Imperial College London Service. TGA was carried out using a Shaimadzu TGA-50 apparatus at a rate of 10 °C min^{-1}.

Preparation of bis(*n*-hexyl(methyl)dithiocarbamato)-platinum(II)/palladium(II)

In a typical synthesis, carbon disulfide (30 cm^3, 15.8 mmol) in 1,4-dioxane (50 cm^3) was added dropwise *via* a dropping funnel to *N*-methylhexylamine (6 cm^3, 15.8 mmol) stirring vigorously in water (120 cm^3) at −10 °C. The solution was filtered and immediately added to sodium tetrachloroplatinate (2.50 g, 7.5 mmol) dissolved in water to give a pale yellow precipitate, which was filtered off and dried under vacuum. The crude product was recrystallised from chloroform at room temperature to give shiny plates of bis(*n*-hexyl(methyl)diselenocarbamato)platinum(II) (2.90 g, 76%), melting point 80 °C (Found: C, 33.61; H, 5.66; N, 4.93; S, 22.34. Calc: C, 33.38; H, 5.60; N, 4.86; S, 22.28%)

NMR: $Pt(S_2CNMe(Hex))_2$: ^1H ($CDCl_3$, 500 MHz), δ 0.89 (3H, t,$(CH_2)_5CH_3$); 1.30 (6H, m, $CH_2CH_2(CH_2)_3CH_3$); 1.77 (2H, m, $CH_2CH_2(CH_2)_3CH_3$); 3.25 (3H, s, CH_3); 3.78 (2H, t, $CH_2(CH_2)_4CH_3$). $^{13}C\{^1H\}$ ($CDCl_3$, 125 MHz), δ 13.96 ($(CH_2)_5CH_3$); 22.43 ($(CH_2)_4CH_2CH_3$); 26.20 ($(CH_2)_3CH_2$-CH_2CH_3); 26.67 ($(CH_2)_2CH_2(CH_2)_2CH_3$); 31.23 (CH_2CH_2-$(CH_2)_3CH_3$); 36.30 (CH_3); 51.60 ($CH_2(CH_2)_4CH_3$); 211.70 (S_2CN).

Bis(*n*-hexyl(methyl)dithiocarbamato)palladium(II) was prepared by same method using sodium tetrachloropalladate. The crude product was recrystallised from hot chloroform, yield: 87%, melting point 85 °C (Found: C, 39.67; H, 6.67; N, 5.82; S, 26.47. Calc: C, 39.45; H, 6.62; N, 5.75; S, 26.33%).

NMR: $Pd(S_2CNMe(Hex))_2$: ^1H ($CDCl_3$, 500 MHz), δ 0.89 (3H, t, $(CH_2)_5CH_3$); 1.29 (6H, m, $CH_2CH_2(CH_2)_3CH_3$); 1.65(2H, m, $CH_2CH_2(CH_2)_3CH_3$); 3.23 (3H, s, CH_3); 3.75 (2H, t, $CH_2(CH_2)_4CH_3$). $^{13}C\{^1H\}$ ($CDCl_3$, 125 MHz), δ 13.95 ($(CH_2)_5CH_3$); 22.44 ($(CH_2)_4CH_2CH_3$); 26.22 ($(CH_2)_3CH_2$-CH_2CH_3); 26.79 ($(CH_2)_2CH_2(CH_2)_2CH_3$); 31.35 (CH_2CH_2-$(CH_2)_3CH_3$); 36.57 (CH_3); 51.47 ($CH_2(CH_2)_4CH_3$); 210.54 (S_2CN).

Preparation of TOPO capped PtS and PdS nanoparticles

TOPO (30 g) was heated under nitrogen to 100 °C in a three-necked flask fitted with condenser and thermometer. The system was then degassed and flushed with nitrogen three times. The temperature was then raised to 250 °C and stabilized at this temperature. $[Pt(S_2CNMe(Hex))_2]$ (1.0 g) was dispersed under stirring in TOP (10 ml) and injected into the TOPO solution through a septum. The reaction was allowed to proceed for 30 min at 250 °C. An excess of methanol was then added to the cooled solution (70 °C), forming a white flocculent precipitate. The solid was separated by centrifugation and re-dispersed in toluene. The pale yellow solution of PtS nanoparticles was evaporated to dryness under vacuum at room temperature. The residue was washed three times with methanol to remove free TOPO, followed by re-dispersion in toluene. The above procedure was repeated for the preparation of TOPO capped PdS nanoparticles, using $[Pt(S_2CNMe(Hex))_2]$ as the single-source precursor.

Growth of PtS or PdS thin films

PtS and PdS films were deposited from $[Pt(S_2CNMe(Hex))_2]$ and $[Pd(S_2CNMe(Hex))_2]$, respectively, using a home made cold-wall low-pressure reactor (10^{-2} Torr) described previously.[14] GaAs substrates were used and these were heated by the action of a quartz halogen lamp on a graphite susceptor. The precursors were held in a tube furnace heated at temperatures in the range 400–500 °C.

Results and discussion

$[Pt(S_2CNMe(Hex))_2]$ is obtained as yellow shiny plates whereas $Pd(S_2CNMe(Hex))_2]$ is a brown microcrystalline solid; neither solid was suitable for X-ray single crystal structure determination. Repeated attempts of recrystallisation to obtain better quality crystals for X-ray structure determination were unsuccessful. Both compounds were used as precursors to synthesise TOPO-capped nanoparticles by injecting a solution of the precursor in TOP into TOPO which was preheated to 250 °C. Thin films of PtS and PdS were grown from both precursors by the MOCVD method.

Optical properties

The optical spectra for a range of nanocrystalline semiconductors show a blue shift in the absorption edge as the particle size decreases. This property of nanoparticles is explained by the confinement of charge carriers within the three dimensions of the particle, allowing quantum size effects to occur. The shifts in the absorption edge for II–VI semiconductors such as CdSe and CdS can result in tuning across a major portion of the visible spectrum. For example the band gap in CdSe can be tuned from 1.7 eV (deep red) to 2.4 eV (green) by reducing the particle size diameter from 200 to 20 Å. The PtS nanoparticles exhibit a strong peak at 360 nm in the absorption spectrum with the band edge at 410 nm (3.02 eV) (Fig. 1). There is no visible excitonic peak in the absorption spectrum of the PdS nanoparticles with the band edge at 455 nm (2.71 eV) (Fig. 2). Both PtS and PdS show broad peaks in their emission spectra. The emission maxima of PtS (495 nm) and PdS (465 nm) are red shifted in relation to their band edges (Figs. 1 and 2). In PtS and PdS the broad shape of the emission spectra is not characteristic of band edge luminescence previously observed for CdS and CdSe.[15–18] This could be due to a broad size distribution of the particles or inefficient passivation of the surface traps by TOPO. However the particle size distribution of both the PtS and PdS nanoparticles as determined by TEM, is narrow. Therefore the broad emission spectrum could be due to recombination from shallow traps, present on the surface, which have not been passivated by TOPO. This type of broad emission spectrum has been previously observed for TOPO capped InS and InSe nanoparticles and also 4-ethylpyridine capped InSe nanoparticles.[19]

Structural properties. Particles in the nanosize regime display broad peaks in their X-ray diffraction spectra and the poor crystallinity of the PtS and PdS nanoparticles is confirmed

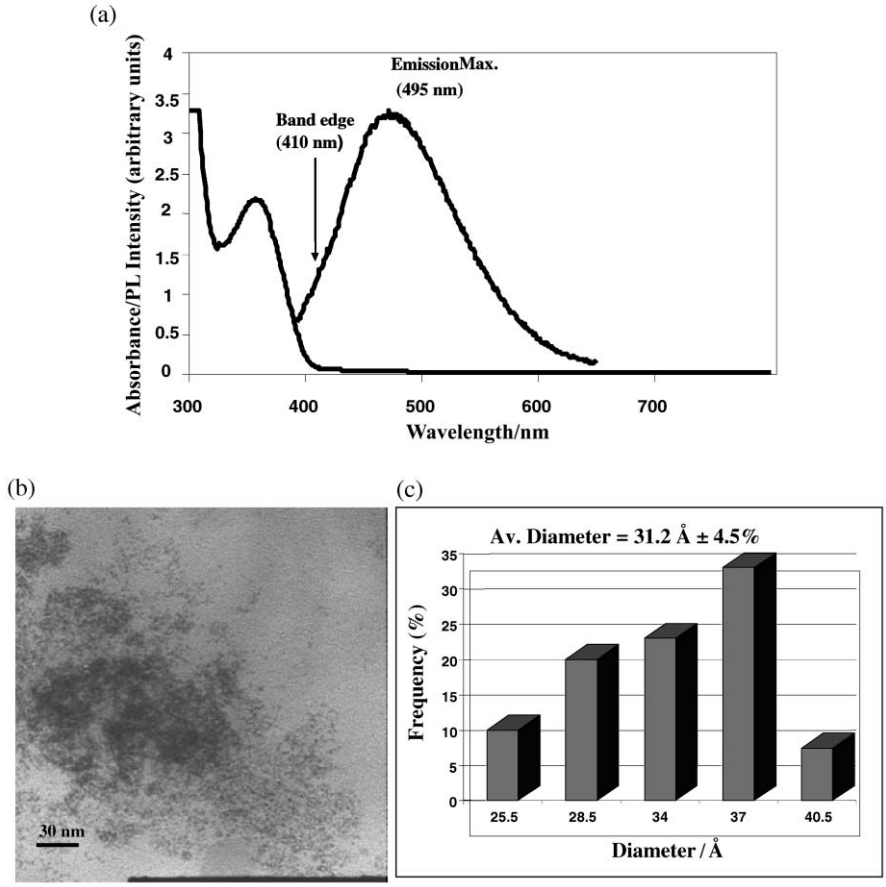

Fig. 1 (a) Absorption (band edge = 410 nm) and emission (emission maximum = 495 nm) spectra of PtS. (b) TEM image of PtS nanoparticles. (c) Particle size distribution (diameter = 31.2 (±4.5%) Å).

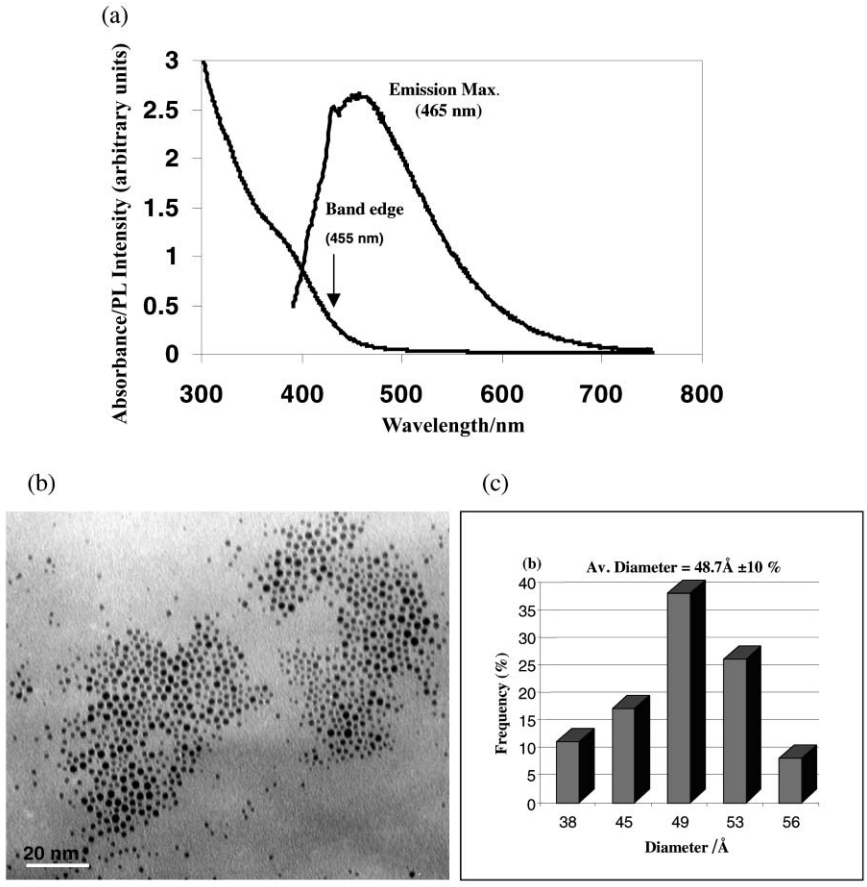

Fig. 2 (a) Absorption (band edge = 455 nm) and emission (emission maximum = 465 nm) spectra of PdS. (b) TEM image of PdS nanoparticles. (c) Particle size distribution (diameter = 48.7(±10%) Å).

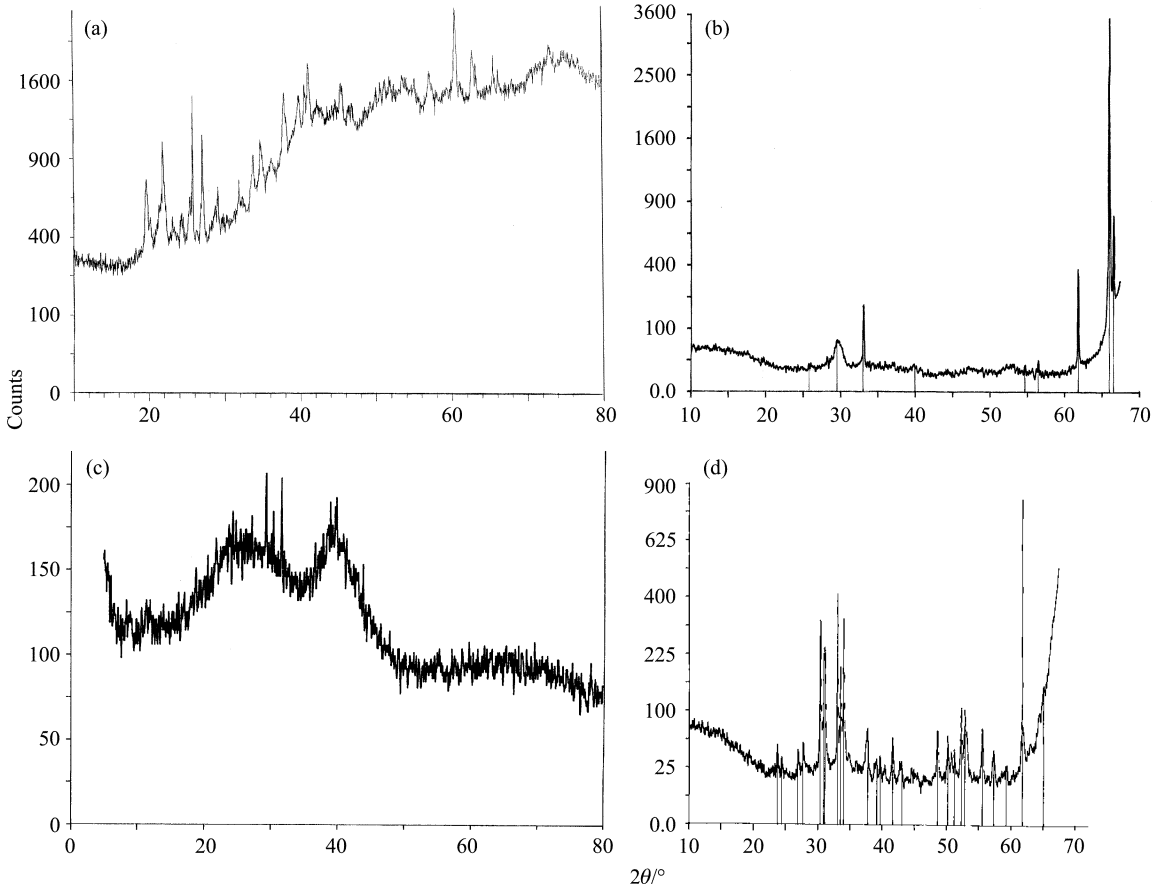

Fig. 3 XRD pattern of (a) TOPO capped PtS nanocrystals, (b) PtS thin film grown on GaAs, (c) TOPO capped PdS nanocrystals and (d) PdS thin film grown on GaAs.

by the broad peaks of their XRD patterns (Fig. 3). The nanometric size regime of the particles was confirmed by the diffuse diffraction rings of the SAED pattern (Fig. 4) which were difficult to index. However, the XRD data for platinum sulfide nanocrystals and thin films can be indexed to a tetragonal phase of PtS and data are given in Table 1. Similarly, palladium sulfide nanoparticles and palladium sulfide thin films grown on GaAs show a tetragonal phase of PdS with XRD data given in Table 2. TEM micrographs of the TOPO capped PtS nanoparticles show particles with sizes in the range 25.5–40.5 Å. The average particle size is 31.2 Å with a narrow size distribution of 4.5% (Fig. 1). In certain areas of the TEM image the particles appear "darker" suggesting a degree of agglomeration. This could be due to the method of sample preparation for TEM, whereby the particles tend to be concentrated in a particular region of the carbon film. However the broad shape of the emission curve suggests that agglomeration of the particles could have occurred before sample preparation. The TEM image of the TOPO capped PdS shows well defined, close to monodisperse particles with an average particle size of

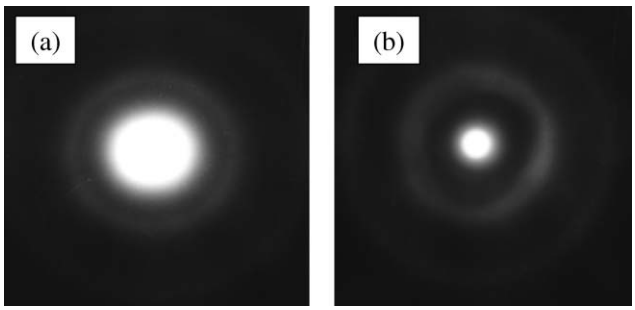

Fig. 4 SAED pattern of (a) PdS and (b) PtS.

Table 1 XRD data for a PtS thin film grown on GaAs and TOPO capped nanoparticles

d(exp.)/Å (thin film)	*d*(exp.)/Å (nanoparticles)	*d*(lit.)[20]/Å	*hkl*
3.45	3.45	3.46	100
3.02	3.06	3.02	101
	2.48	2.46	110
	1.93	1.91	112
	1.76	1.75	103
	1.73	1.73	200
1.50	1.53	1.53	004
	1.48	1.50	211
	1.33	1.30	114

Table 2 XRD data for a PdS thin film grown on GaAs and TOPO capped nanoparticles

d(exp.)/Å (thin film)	*d*(exp.)/Å (nanoparticles)	*d*(lit.)[20]/Å	*hkl*
3.75	3.75	3.75	111
3.31	3.32	3.31	002
3.21	3.20	3.21	200
2.94	2.95	2.95	102
2.89		2.89	201
2.67		2.68	112
2.64		2.64	121
2.31	2.31	2.31	202
2.26	2.26	2.27	220
2.17	2.17	2.17	122
1.87		1.87	222
1.82		1.82	203
1.75		1.75	123
1.73		1.73	312
1.65		1.66	004
1.61		1.61	400
1.43		1.44	124

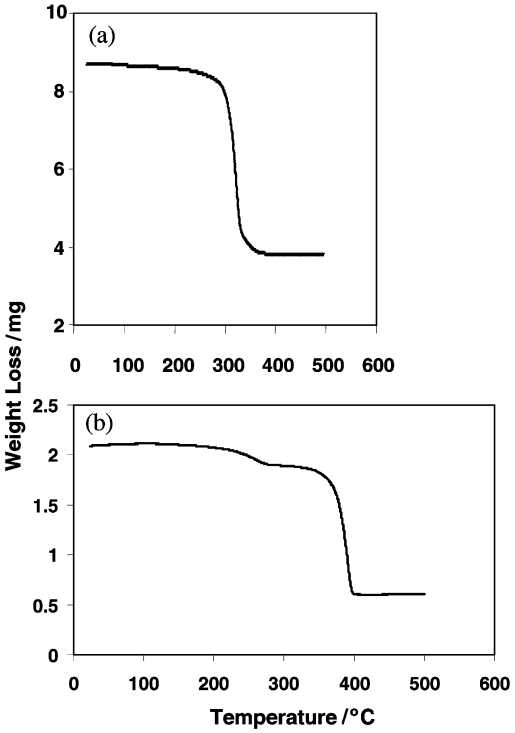

Fig. 5 TGA analysis of (a) bis(*n*-hexyl(methyl)dithiocarbamato)palatinum(II) which sublimes between 320 and 380 °C and then decomposes leaving a 45 wt% residue and (b) bis(*n*-hexyl(methyl)dithiocarbamato)palladium(II) which sublimes between 380 and 400 °C and then decomposes leaving a 25 wt% residue.

48.7 Å (±10%) (Fig. 2). The particles appear well spaced out on the grid with no evidence of agglomeration. The EDAX pattern of PtS nanoparticles showed the presence of Pt, S and P, while PdS showed the presence of Pd, S and P. The peak for phosphorus in each case was due to the capping of the particles by TOPO which was further confirmed by a shift in the IR band (from $\nu = 1146$ to 1120 cm^{-1}) for TOPO.

Thin films

PtS and PdS thin films were grown onto GaAS substrates using bis(*n*-hexyl(methyl)dithiocarbamato)platinum(II) and bis(*n*-hexyl(methyl)dithiocarbamato)palladium(II), respectively. Deposition experiments were carried out at various deposition temperatures, *i.e.* 400–500 °C, but the films were grown only at 500 °C. No growth was observed at temperatures lower than 500 °C in both cases. Thermogravimetric analysis (TGA) showed

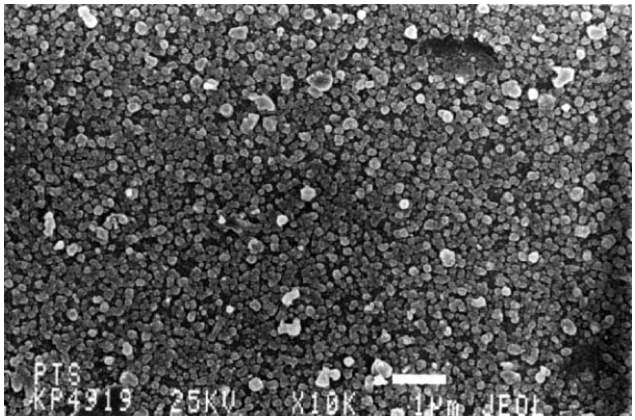

Fig. 6 SEM micrograph of PtS grown on GaAs at 500 °C.

that the bis(*n*-hexyl(methyl)dithiocarbamato)platinum(II) complex started subliming at *ca.* 320 °C and decomposed at *ca.* 380 °C (Fig. 5(a)). No growth occurred below a precursor temperature of 350 °C. Bis(*n*-hexyl(methyl)dithiocarbamato)-palladium(II) started subliming at *ca* 380 °C and decomposed at 400 °C (Fig. 5(b)).

Scanning electron microscopy (SEM) showed that the films grown over a period of 1 h were very thin with a crystallite size of 0.1 μm for PtS (Fig. 6) and 0.2 μm for PdS (Fig. 7). EDAX patterns confirmed the presence of Pt and S in PtS films and Pd and S in PdS films. XRD patterns showed tetragonal phases of PtS and PdS (Fig. 3). XRD data are given in Table 1 for PtS and Table 2 for PdS.

Conclusion

Two new compounds, bis(*n*-hexyl(methyl)dithiocarbamato)-platinum(II) and bis(*n*-hexyl(methyl)dithiocarbamato)palladium(II) have been synthesised and characterised.

Both complexes have been used as precursors to grow thin films of PtS and PdS, respectively, on to GaAs substrates by the low pressure metal organic chemical vapour deposition (LP-MOCVD) method. The films grown were characterised by XRD, EDAX and SEM methods. These complexes appear to be less volatile when compared to the corresponding zinc or cadmium complexes and hence require higher deposition temperature with slower growth rates. However, these complexes are useful precursors for the growth of nanocrystals of PtS or PdS by thermolysis in tricotylphosphine oxide (TOPO) where volatility of the precursors is not a requirement. TOPO capped mono-dispersed nanoparticles of PtS (*ca.* 3 nm diameter) and PdS (*ca.* 5 nm diameter) were prepared using the

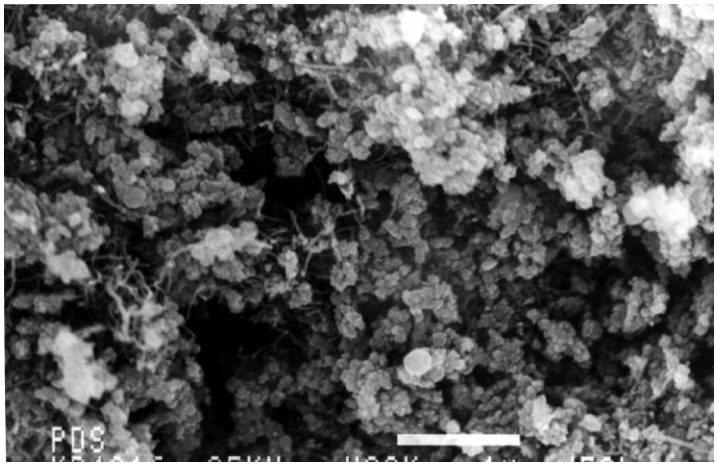

Fig. 7 SEM micrograph of PdS grown on GaAs at 500 °C.

corresponding precursors. The PtS nanoparticles exhibit a strong excitonic peak at 360 nm in the absorption spectrum with the band edge at 410 nm. There is no visible excitonic peak in the absorption spectrum of the PdS nanoparticles with the band edge at 455 nm. Both PtS and PdS show broad peaks in their emission spectra. The emission maxima of PtS (495 nm) and PdS (465 nm) are red shifted in relation to their band edges. XRD patterns showed both PtS and PdS to be tetragonal phases. The TEM image of the TOPO capped PdS shows well defined, close to monodispersed particles with an average particle size of *ca* 5 nm. The particles appear well spaced out on the grid, with no evidence of agglomeration. The EDAX spectra show the presence of palladium and sulfur or platinum and sulfur with, in each case, a strong peak for phosphorus due to TOPO.

Acknowledgements

We thank the Royal Society and the National Research Foundation (NRF) for support to N. R. and a program of collaboration between UZULU and ICSTM. P. O'B. thanks the EPSRC for a grant. P. O'B. is the Sumitomo/STS visiting Professor of Materials Chemistry at IC.

References

1 L. Y. Chiang, T. Swirczewski, R. Kastrup, C. S. Hsu and R. B. Upasani, *J. Am. Chem. Soc.*, 1991, **113**, 6574.
2 S. Eijsbouts, V. H. J. De Beer and R. Prins, *J. Catal.*, 1988, **109**, 217.
3 M. Misono and N. Nojiri, *Appl. Catal.*, 1990, **64**, 1.
4 J. J. Bladon, A. Lamola, F. W. Lytle, W. Sonnenberg, J. N. Robinson and G. Philipose, *J. Electrochem. Soc.*, 1996, **143**, 1206.
5 C. H. Yang, Y. Y. Wang, C. C. Wan and C. J. Chen, *J. Electrochem. Soc.*, 1996, **143**, 3521.
6 T. Yamamoto, *Chem. Abstr.*, 1987, **106**, 8769h.
7 T. Oota, K. Yoshioka, T. Akyama and S. Mori, *Chem. Abstr.*, 1995, **123**, 325855j.
8 K. Nakamoto, J. Fujita, R. A. Condrate and Y. Morimoto, *J. Chem. Phys.*, 1963, **39**, 423.
9 I. B. Rufus, B. Viswanathan, V. Ramakrishnan and J. C. Kuriacose, *J. Photochem. and Photobiology A-Chem.*, 1995, **91**, 63.
10 *Dictionary of Inorganic Compounds*, vol.3, IC.-017115.
11 *Dictionary of Inorganic Compounds*, vol.3, IC.-021806.
12 T. Yamamoto, A. Taniguchi, S. Dev, E. Kubota, K. Osakada and K. Kubota, *Colloid Polym. Sci,*, 1991, **269**, 969.
13 A. Singhal, V. K. Jain, R. Mishra and B. Varghese, *J. Mater. Chem.*, 2000, **10**, 1121.
14 M. A. Malik and P. O'Brien, *Adv. Mater. Opt. Electron.*, 1994, **3**, 171.
15 U. Banin, M. Bruchez, A. P. Alivisatos, T. Ha, S. Weiss and D. S. Chemia, *J. Chem. Phys.*, 1999, **110**, 119.
16 B. Ludolph, M. A. Malik, N. Revaprasadu and P. O'Brien, *Chem. Commun.*, 1998, 1849.
17 C. B. Murray, D. J. Norris and M. G. Bawendi, *J. Am. Chem. Soc.*, 1993, **115**, 8706.
18 X. G. Peng, J. Wickham and A. P. Alivisatos, *J. Am. Chem. Soc.*, 1998, **120**, 5343.
19 N. Revaprasadu, M. Azad Malik, J. Carstens and P. O'Brien, *J. Mater. Chem.*, 1999, **9**, 2885.
20 Joint Committee on Powder Diffraction Standards (JCPDS), 1999, 74–1060, 02–0642.